



Polyhydroxybutyrate (PHB) produced from red grape pomace: Effect of purification processes on structural, thermal and antioxidant properties

Alaitz Etxabide^{a,b,*}, Paul A. Kilmartin^b, Pedro Guerrero^{a,c}, Koro de la Caba^{a,c}, David O. Hooks^d, Mark West^d, Tripti Singh^d

^a BIOMAT Research Group, University of the Basque Country (UPV/EHU), Escuela de Ingeniería de Gipuzkoa, Plaza de Europa 1, 20018 Donostia-San Sebastián, Spain.

^b School of Chemical Sciences 302, University of Auckland, 23 Symonds Street, Private Bag 92019, 1010 Auckland, New Zealand.

^c BCMaterials, Basque Center for Materials, Applications and Nanostructures, UPV/EHU Science Park, 48940 Leioa, Spain.

^d Wood Science Design Scion, 49 Sala Street, Private Bag 3020, 3010 Rotorua, New Zealand.

ARTICLE INFO

Keywords:

Grape pomace
PHB
Extraction
Purification
Characterization
Antioxidant activity

ABSTRACT

Red grape pomace was used as a source for poly(3-hydroxybutyrate) (PHB) production, which was then subject to a range of purification processes. The different PHB biopolymers were characterized for chemical structure, crystallinity, thermal properties, colour, release of compounds into different food simulants and antioxidant inhibition, and comparisons were made with a commercially available PHB. An increase in purification steps did not have a significant effect on the high thermal stability of the extracted biopolymer, but it decreased the degree of crystallinity and the presence of amino acids and aromatic compounds. With additional purification, the PHB powders also whitened and the number of components released from the biopolymer into food simulants decreased. The released compounds presented antioxidant inhibition, which has not been previously reported in the literature or with commercially available polyhydroxyalkanoates. This is of great interest for food packaging and biomedical industries where the addition of antioxidant additives to improve PHB functional properties may not be necessary and could be avoided.

1. Introduction

The interest to use renewable and biodegradable polymers, such as collagen and chitin, extracted from fishery by-products, and soy protein and polyesters obtained from agriculture by-products, has grown in the last decades. This is due to the urgent need to replace petroleum-derived synthetic plastics, which are non-renewable and non-biodegradable, and have resulted in significant waste accumulation (mainly single-use food packaging wastes), and to gain an economic advantage in production costs from the use of inexpensive industrial by-products [1–5].

On this matter, 40,323 ha were used for wine production in 2021 in Aotearoa New Zealand, with Marlborough the largest wine-producing region (around 70 % of the total producing area). Vine prunings, grape stalks and marc are waste-streams generated in the production of wine [6,7]. It is estimated that grape marc accounts for 20 % of the total weight of the fruit of the grape, which represents a challenging waste disposal problem for the wine industry.

Grape marc, also named grape pomace, is a solid by-product

composed mainly of polysaccharides (30 %), as well as other compounds such as acid pectic substances, lignin, and proteins, in lesser percentages [8]. It also contains considerable quantities of phenolics, flavonoids and anthocyanins with high antioxidant potential. Furthermore, it has been shown that the sugars present in the marc can be used as carbon sources for the industrial production of polyhydroxyalkanoates (PHAs) [9,10].

PHAs represent a class of biopolymers, microbiologically produced polyesters, that are renewable and completely biodegradable to CO₂, water and biomass. PHAs are an interesting solution to tackle the issues caused by synthetic polymers. When isolated from microbial biomass, PHAs have shown similar physical properties as synthetic polymers. For example, polyhydroxybutyrate (PHB), a member of the PHA family, closely resembles common synthetic polymers such as polyethylene (PE) and polypropylene (PP) [11,12]. PHAs are also biocompatible materials, making these polymers suitable for biomedical applications. For example, PHB exhibits low toxicity as in vivo it degrades to D-3-hydroxybutyric acid, which is a normal human blood constituent. These

* Corresponding author at: BIOMAT Research Group, University of the Basque Country (UPV/EHU), Escuela de Ingeniería de Gipuzkoa, Plaza de Europa 1, 20018 Donostia-San Sebastián, Spain.

E-mail address: alaitz.etxabide@ehu.es (A. Etxabide).

<https://doi.org/10.1016/j.ijbiomac.2022.07.072>

Received 19 May 2022; Received in revised form 5 July 2022; Accepted 9 July 2022

Available online 13 July 2022

0141-8130/© 2022 The Authors. Published by Elsevier B.V. This is an open access article under the CC BY-NC-ND license (<http://creativecommons.org/licenses/by-nc-nd/4.0/>).

characteristics make PHAs promising candidates as a substitute for conventional synthetic polymers in a broad range of applications in different sectors. These include biodegradable (single-use) food packaging and biomaterials (sutures, patches, scaffolds for tissue regeneration, controlled drug-release devices), among others [11,13].

In this study, red grape pomace was used as a source of PHB production. Moreover, unlike other research works, the obtained PHB was purified under different purification processes before characterization for structure, crystallinity, thermal properties, and colour, with comparisons made to literature values and to a commercially available PHB. Furthermore, the effect of PHB purification processes on the release of bioactive compounds into various food simulants and their antioxidant activity were also analysed. These latter characterizations do not appear to have been previously reported in the literature or for commercially available PHAs [14].

2. Materials and methods

2.1. Materials

Red grape pomace was obtained from a vineyard in Marlborough. CTec2 enzyme was manufactured by Novazyme (Denmark), while *Cupriavidus necator* H 1 G⁺3 bacteria (DSM 454) was obtained from the DSMZ (Germany). The poly(3-hydroxybutyrate) (PHB) used for comparisons was supplied by Biomer (Schwalbach, Germany). Chemicals, (NH₄)₂SO₄, Na₂HPO₄·2H₂O, KH₂PO₄, MgSO₄·7H₂O, Tris-HCl, EDTA, SDS and 2,2-diphenyl-1-picryl hydrazyl (DPPH), were purchased from Sigma-Aldrich. Ethanol and methanol were obtained from ECP Lab-Chem, and chloroform and the yeast extract were purchased from Applichem.

2.2. Biomass, microbial strain preparation and PHB biosynthesis/production

Red grape pomace (150 g) was mixed with reverse osmosis (RO) water (300 mL) and heated at 50 °C. Then, 15 g of CTec2 enzyme was added and the mixture was blended for 4 min. The blend was centrifuged (10,000 g, 30 min), before the supernatant was decanted and subject to pasteurization (at 70 °C for 2 h). The final concentration of the pomace (named saccharified grape pomace) contained 17 g/L (25.5 g/100 g pomace) and 7.2 g/L (10.8 g/100 g pomace) of glucose and fructose, respectively.

Cupriavidus necator H 1 G⁺3 bacteria strain was used in this work. The bacteria growth was carried out using the saccharified grape pomace and the following recipe named YEM [15]: 1.0 g (NH₄)₂SO₄, 4.5 g Na₂HPO₄·2H₂O, 1.5 g KH₂PO₄, 0.2 g MgSO₄·7H₂O, 1.0 g yeast extract, and 1 mL trace elements in 1 L RO water. The *Cupriavidus necator* culture was first grown at 30 °C and 200 rpm for 24 h, and the grape pomace was inoculated with the culture in YEM at 30 °C and 200 rpm for 48 h. Glucose and fructose were not detected in the final culture, and approximately 20 g of cell pellet was recovered from the 1 L culture.

2.3. PHB extraction and purification

The cell pellets were resuspended in Tris-HCl EDTA (TE) 5 % SDS (w/v) buffer, passed 3 times through ice-cooled on HPH at maximum pressure (10 min/L), and washed 3 times in 20 % ethanol by centrifugation (8000g, 20 min, 10 °C). Approximately 4 g of dried material was recovered from the 20 g cell pellets.

A powder of 66 % PHB mixed with cell materials was obtained (named PHB66, molecular weight (Mw) 1.2 × 10⁶ g/mol, dispersity (D) = 2.8). The PHB66 was then washed with ethanol (EtOH) to remove the soluble cells materials, and a powder was obtained with 85 % PHB (named PHB85, Mw 1.1 × 10⁶ g/mol, D = 2.6). Some of this powder was dissolved in chloroform (CHCl₃), precipitated in methanol and filtered to obtain a film like PHB (named PHB95, 95 % PHB, Mw 3.8 × 10⁵ g/

mol, D = 2.9). The 3 different PHBs were analysed and compared with a commercially available PHB (named PHBcom, 98.5 % PHB, Mw 3–6 × 10⁵ g/mol).

2.4. PHB characterization

2.4.1. Nuclear magnetic resonance (¹H NMR) spectroscopy

¹H NMR spectroscopy was used to determine the chemical structure and purity of the extracted polymer samples. 5 mg of a PHB were dissolved in 0.6 mL CDCl₃. The spectra were recorded on a Bruker Avance III 400 MHz instrument.

2.4.2. Fourier transform infrared (FTIR) spectroscopy

FTIR spectra of the PHBs were obtained using a Bruker Vertex 70 FTIR spectrometer with Platinum Diamond Micro-ATR accessory (Bruker Optics, New Zealand). The samples were placed directly onto the ATR crystal and spectra were collected in transmittance mode. Each spectrum was a result of the average of 32 scans performed at 4 cm⁻¹ resolution, and the measurements were recorded between 4000 and 450 cm⁻¹ at room temperature.

2.4.3. X-ray diffraction (XRD) analysis

X-ray diffraction studies of the PHBs were performed using a diffraction unit (Empyrean, Malvern Panalytical, Cleveland, New Zealand) operating at 45 kV and 40 mA. The radiation was generated from a Cu-Kα (λ = 1.5418 Å) source. The diffraction data of the samples were collected from 2θ values from 10° to 35°, where θ is the incidence angle of the X-ray beam on the sample.

The crystallinity index (CrI) of the PHB samples was calculated following the formula suggested by Wei and co-workers [16]:

$$CrI (\%) = \frac{I_{17}}{I_{Total}} \times 100$$

where I₁₇ is the intensity of the peak close to 2θ = 17° and I_{Total} is the total intensity of all crystalline peaks of the PHB. It has been reported in the literature that CrI is useful to make general comparisons between the samples; however, it is not an absolute value for determining the crystallinity of PHB [17].

2.4.4. Thermogravimetric analysis (TGA)

Thermo-gravimetric measurements were performed using a TA Instruments system (Q5000, Alphatec Systems Limited, Auckland, NZ). PHB samples (3.2 ± 0.4 mg) were tested from 25 °C up to 600 °C at a heating rate of 10 °C/min under a nitrogen atmosphere (25 mL/min) to avoid thermo-oxidative reactions.

2.4.5. Differential scanning calorimetry (DSC)

DSC measurements were performed using a TA Instruments system (Q1000, Alphatec Systems Limited, Auckland, NZ) equipped with an electric intercooler as a refrigeration unit. Samples (3.1 ± 0.4 mg) were hermetically encapsulated in aluminium pans to prevent mass loss during heating from 25 to 200 °C at a rate of 10 °C/min, cooling to -50 °C at a rate of 5 °C/min, and heating to 200 °C at a rate of 10 °C/min under inert atmosphere conditions (30 mL/min N₂). The crystallinity of PHB was estimated from the enthalpy of fusion (melting enthalpy). For this determination, the enthalpy of fusion of a 100 % crystalline (theoretical) sample was assumed to be 146.6 J/g [18,19].

2.4.6. Colour of the PHB samples

Sample colour was determined using a CR-300 Minolta colourimeter (Konica Minolta, Japan) previously calibrated on a white standard calibration plate. Samples were placed onto the surface of a white plastic tray (L* 91.28, a*1.4 and b* -3.31) and then, L*, a* and b* colour parameters were measured using the CIELAB colour scale: L* = 0 (black) to L* = 100 (white), -a* (greenness) to +a* (redness), and -b*

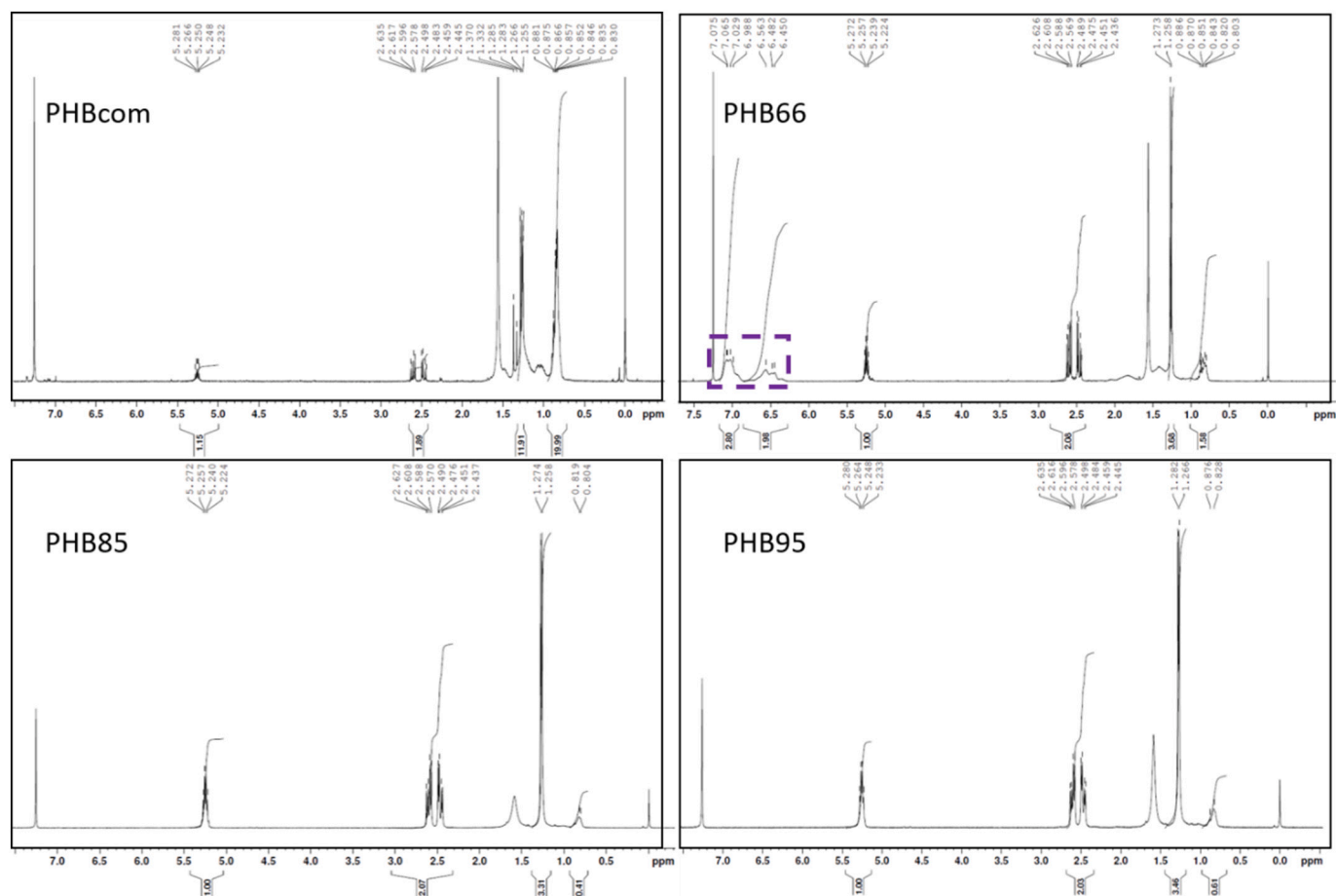


Fig. 1. ^1H NMR spectra of extracted (PHB66) and successively purified (PHB85 and PHB95) PHB samples. A commercial PHB (PHBcom) was used for comparison.

(blueness) to + b* (yellowness). The CIELAB colour system was converted into RGB units to display the approximate colour of the samples. Data were subjected to a one-way analysis of variance (ANOVA) through an SPSS computer program (SPSS Statistic 25.0). Post hoc multiple comparisons were determined by Tukey's test with the level of significance set at $P < 0.05$. The minimum number of replications for each sample was 9.

2.4.7. Release of compounds from PHB samples

The migration of components depends on the food matrix, which can be simulated using different food simulants. The selection of the food simulants was carried out by analysing the migration of compounds from PHB66 in 3 different food simulants: Milli-Q water (MQW) for hydrophilic foods, and 50 % v/v ethanol (50EtOH) and 95EtOH for lipophilic foods [20]. Hence, 5 mL of a food simulant was added to 5 mg of PHB66 (1 mg/mL) and the solution was left under stirring (250 rpm) for 24 h at 25 °C. The solution was then centrifuged at 1000 rpm for 5 min and the supernatant liquid was analysed within quartz cuvettes at a NanoPhotometer (NP80, IMPLLEN, Europe), recording wavelengths from 200 to 800 nm. Three samples ($n = 3$) were analysed for each composition. The release of antioxidant compounds from the other PHB samples (PHB85, PHB95 and PHBcom) was carried out in MQW (due to the hydrophilic character of the aromatic impurities) following the same procedure explained above.

2.4.8. Antioxidant activity (DPPH assay)

The DPPH test is used for the assessment of the free radical scavenging potential of a molecule and is considered one of the standard methods for the assessment of antioxidant activity [21]. In this study, the DPPH radical scavenging activity was measured in the liquid (1 mg

PHB/1 mL MQW) samples ($n = 3$) obtained in Section 2.4.7, according to the procedure carried out in a previous work [22]. The inhibition values were determined by the absorbance decrease at 517 nm as follows:

$$\text{Inhibition (\%)} = \frac{A_c - A_s}{A_c} \times 100$$

where A_c is the absorbance of the MQW and A_s is the absorbance of the MQW in which the PHB samples were immersed.

3. Results and discussion

3.1. ^1H NMR

The chemical structure of *Cupriavidus necator* H 1 G⁺3 produced PHB was analysed by ^1H NMR (Fig. 1). Three signals, characteristic of the PHB polymer, were observed at around $\delta = 1.25$, 2.50, and 5.25 ppm, which correspond to the methyl groups (-CH₃), methylene groups (-CH₂), and methane groups (-CH) of PHB, respectively. Similarly, Tra-kunjae and colleagues [23] produced PHB using a *Rhodococcus pyridinivorans* strain BSRT1–1, and the ^1H NMR spectrum showed 3 different signals at $\delta = 1.29$, 2.50, and 5.27 ppm, which represent the methyl, methylene, and methane groups, respectively. In a study conducted by Narayanan and co-workers [24] on a *Bacillus cereus* produced PHB, 3 signals at $\delta = 2.37$, 2.55 and 3.39 ppm were found and related to -CH₃, -CH₂, and -CH groups, respectively. The ^1H NMR results of the extracts were identical to those for the PHB standard and so, it was concluded that the PHA synthesized by strain *Cupriavidus necator* H 1 G⁺3 was indeed PHB [25,26]. The peaks around $\delta = 0$ ppm, $\delta = 1.56$

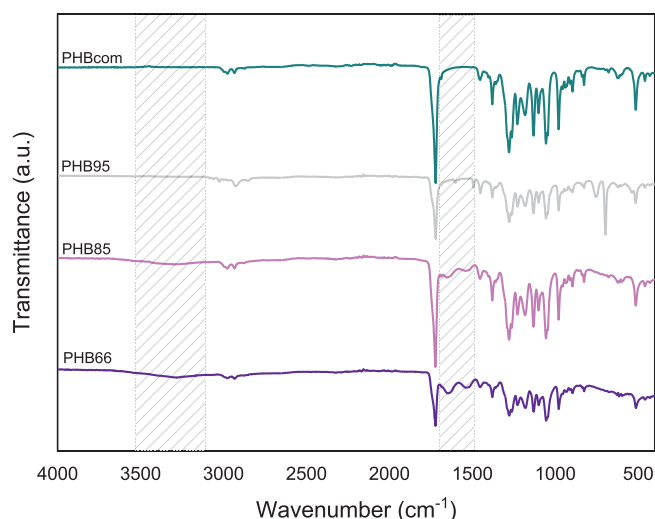


Fig. 2. FTIR spectra of extracted (PHB66) and successively purified (PHB85 and PHB95) PHB samples. A commercial PHB (PHBcom) was used for comparison.

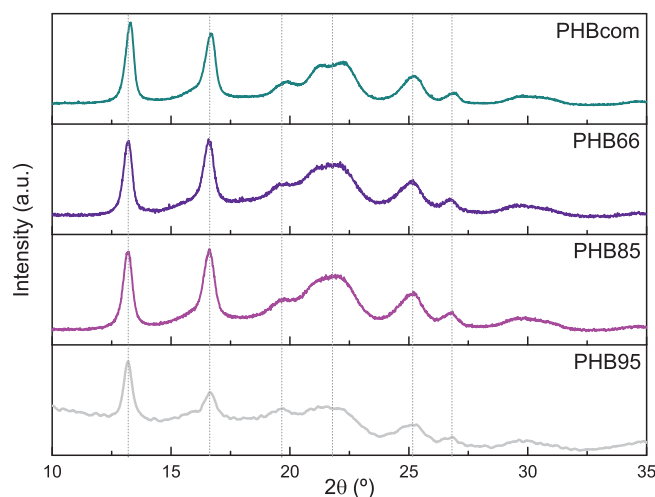


Fig. 3. XRD patterns of extracted (PHB66) and successively purified (PHB85 and PHB95) PHB samples. A commercial PHB (PHBcom) was used for comparison (the Y axes do not have the same scale in each sample).

ppm and $\delta = 7.26$ ppm represent tetramethylsilane ($(\text{CH}_3)_4\text{Si}$), water (H_2O), and the solvent (CD_3Cl), respectively. Unlike PHB85 and PHB95, in PHB66, additional signals were seen around $\delta = 7.00$ ppm and $\delta = 6.50$ ppm, which can be related to aromatic impurities such as gallic acid (a phenolic acid, $\delta \sim 7.1$ ppm) and tyrosine (an aromatic amino acid, $\delta \sim 6.7$ ppm), found in by-products of the winemaking process (grape pomace extracts) [27] as well as in dry red wines [28].

3.2. Fourier transform infrared (FTIR) spectroscopy

The functional groups of the *Cupriavidus necator* H 1 G⁺3 produced PHB were analysed by FTIR (Fig. 2). The characteristic bands at 2975 and 2935 cm^{-1} were related to the presence of $-\text{CH}_3$ (methyl) and $-\text{CH}_2$ (methylene) groups, respectively. The band at 1722 cm^{-1} was associated with the $\text{C}=\text{O}$ (ester carbonyl) group, while the fingerprint region at 800–1500 cm^{-1} included stretching vibrations of $\text{C}-\text{CH}$, $\text{C}-\text{CH}_3$, $\text{C}-\text{O}$, and $\text{C}-\text{C}$ bonds [1,5]. The FTIR spectra of the extracted and purified PHB samples matched closely the commercial PHB, confirming that the synthesized PHA was PHB [29]. However, some differences were

Table 1

2θ and intensity values of all crystalline peaks of extracted and purified PHB samples and their crystallinity index (CrI) values. A commercial PHB (PHBcom) was used for comparison.

PHBcom		PHB66		PHB85		PHB95	
2θ (°)	Intensity (a.u.)	2θ (°)	Intensity (a.u.)	2θ (°)	Intensity (a.u.)	2θ (°)	Intensity (a.u.)
13.29	10,139	13.21	4,510	13.21	5,316	13.21	966
16.68	8,932	16.64	4,466	16.64	5,399	16.64	702
19.87	3,388	19.66	2,427	19.66	2,566	19.66	565
21.75	5,151	21.79	3,247	21.79	3,941	21.79	557
25.24	4,099	25.18	2,477	25.18	3,031	25.18	386
27.90	939	27.77	1,140	27.77	1,091	27.77	211
CrI (%)	27.36	CrI (%)	24.45	CrI (%)	25.30	CrI (%)	20.73

observed depending on the PHB purification level. PHB66 samples showed a small band at ~ 3300 cm^{-1} , which corresponds to $\text{O}-\text{H}$ stretching (moisture/water), and two bands at 1643 and 1563 cm^{-1} that might indicate the presence of amino acids [30] and phenolic compounds [31], consistent with the ^1H NMR results. The presence of these bands decreased in the PHB85 sample, while they were not visible in the further purified PHB95 sample. These FTIR results, along with ^1H NMR outcomes, showed that the degree of purity of the extracted PHBs increased as follows: PHB95 > PHB85 > PHB66. This matched the purification processes undertaken with each sample (none), PHB85 (washing with EtOH), PHB95 (dissolution in CHCl_3 , precipitation in methanol and filtration).

3.3. XRD

The crystalline structure of the extracted and purified PHB samples was studied by XRD (Fig. 3). Distinctive peaks for PHB were observed at 2θ values of 13.21° and 16.64°, attributed to (020) and (110) planes, which indicated the crystalline structure of the biopolymer; at $2\theta = 19.66^\circ$ and 21.79°, attributed to (101) and (111) planes, which indicated the presence of orthorhombic crystals; and low-intensity peaks at $2\theta = 25.18^\circ$ and 27.77°, attributed to the (121) and (040) planes, which indicated the partial crystalline nature of PHB [17,32,33]. These XRD patterns of the samples agreed with the pattern of the PHBcom ($2\theta = 13.29^\circ$, 16.68°, 19.87°, 21.75°, 25.24° and 27.90°) used for comparison. The intensity, and so the crystallinity index of the peaks (Table 1), differed as a function of the PHB purification process, especially for the purest PHB (PHB95), which showed the lowest crystalline index value (close to 21%). Similar values were found by Mat3nez-Herrera and colleagues [17] on PHB extracted from *Bacillus cereus* 4 N, where the CrI values of extracted biopolymers were around 22% compared to a commercial PHB (near 29%). The crystallinities of PHB obtained in this study were also lower than the PHBcom ($\sim 27\%$). A lower crystallinity in polymers is linked to less brittle properties [32,34], so it increases the range of applications of the PHB-based material.

3.4. TGA

The PHB degradation pattern of extracted and purified samples showed a single-stage decomposition, marked by a sharp decrease in the curve between ~ 280 °C (onset) and ~ 340 °C (offset), which indicated that PHB degradation occurred rapidly (Fig. 4). The dominant mechanism of PHB thermal degradation has been considered to be $\text{C}=\text{O}$ and $\text{C}-\text{O}$ bonds scission by β -elimination in ester moieties, which leads to oligomeric acids and finally crotonic acid with a decrease in the molecular weight [35]. Nevertheless, there were suggestions that other reactions besides the scission occur during PHB degradation, [36]. Unlike the other PHB samples, the PHB95 sample presented a second degradation step at ~ 440 °C (total mass loss of around 95%). This result may be related to the purification processes of PHB95 (dissolution in CHCl_3 , precipitation in methanol and filtration), which could induce changes in the polymer chain reorganization. In fact, these changes led

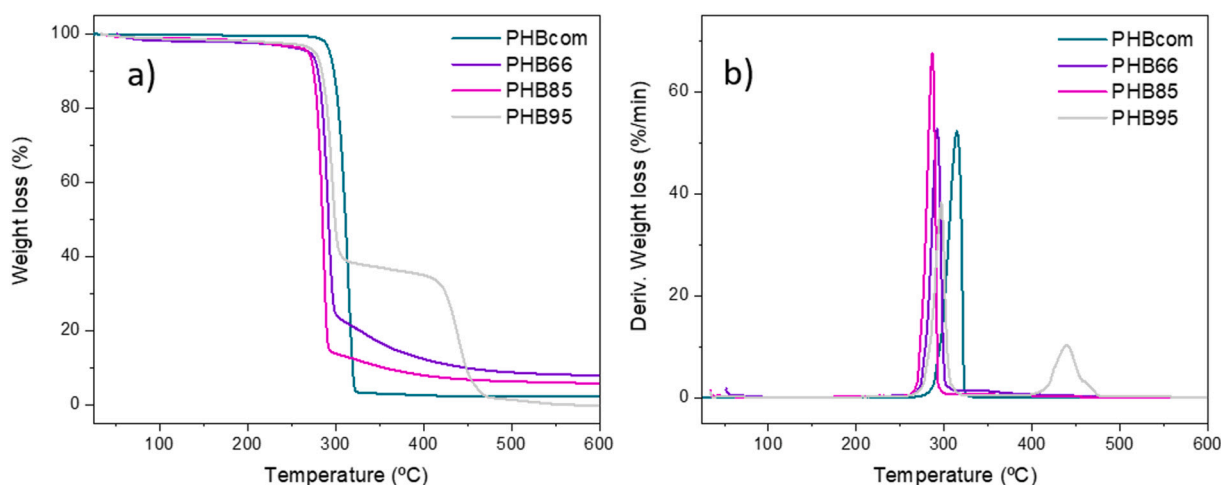


Fig. 4. a) TGA and b) TGA derivative (Deriv.) thermograms of extracted (PHB66) and successively purified (PHB85 and PHB95) PHB samples. A commercial PHB (PHBcom) was used for comparison.

Table 2

Onset temperature (T_{onset}) and its mass loss at stage 1 (S1) and stage 2 (S2); maximum thermal decomposition (T_{max}) and its mass loss; and residual mass at 600 °C of extracted (PHB66) and successively purified (PHB85 and PHB95) PHB samples while thermal degradation. A commercial PHB (PHBcom) was used for comparison.

Sample	T_{onset} (°C)	Mass loss (%) at T_{onset}	T_{max} (°C)	Mass loss (%) at T_{max}	Residual mass (%) at 600 °C
PHB66	283	75	292	50	7.83
PHB85	279	83	286	60	5.68
PHB95	287/ (S1/S2)	59/34	297/ 440	42/82	0

Table 3

The values of melting (T_m), crystallization (T_c), and glass transition (T_g) temperatures, T_m and T_c enthalpies, and the crystallinity degree (X_c) obtained using DSC analysis for extracted (PHB66) and successively purified (PHB85 and PHB95) PHB samples. A commercial PHB (PHBcom) was used for comparison^a.

Sample	Heating				Cooling	
	T_g (°C)	T_{m1}/T_{m2} (°C)	$\Delta H_1/\Delta H_2$ (J/g)	X_{c1}/X_{c2} (%)	T_c (°C)	ΔH (J/g)
PHBcom	2.3	174.9/ 172.0	75.8/74.9	51.7/51.1	97.8	84.0
PHB66	-3.1	175.0/ 166.7	46.5/ 48.18	31.7/32.9	91.5	56.3
PHB85	4.81	174.9/ 164.5	64.5/68.1	44.0/46.5	102.4	78.2
PHB95	4.93	175.4/ 167.2	46.4/46.7	31.7/31.9	98.5	49.3

^a 1 and 2 mean the number of the heating cycle.

the inflexion point in the TGA curve or the peak at the DTG curve) and its mass loss were observed at ~314 °C and ~66 % for PHBcom, ~292 °C and ~50 % for PHB66, ~286 °C and ~60 % for PH85, and ~297 °C and ~42 % for PHB95. These T_{max} values indicated that the produced biopolymer had high thermal stability [33]. Similar results were obtained by Pradhan and colleagues [11] on PHB from *P. hysterothorus* and *E. crassipes*. Regarding the residual mass at 600 °C, the remaining inorganic fraction decreased as the purification of PHB increased. The variations in T_{onset} , T_{max} , mass losses, and the remaining residual material could be related to differences in the purification processes (and so, the purity of the PHBs), morphology (crystallinity), and Mw of the samples, as reported in the literature [11,17,37].

3.5. DSC

The melting and crystallization behaviours of PHBs samples were investigated using DSC (Fig. 5). The values for the main thermal events, such as the melting (T_m), crystallization (T_c), and glass transition (T_g) temperatures, T_m and T_c enthalpies, and the crystallinity degree (X_c) calculated from T_m , are reported in Table 3. The extracted and purified PHBs showed T_m and T_c values of around 170 and 95 °C, respectively, which closely matched with the T_m and T_c of the PHBcom. It is worth mentioning that, unlike the PHBcom, in the extracted and purified PHB samples, the peak related to T_m showed one or two crystalline melting peaks with different intensities before (heating cycle 1) and after (heating cycle 2) crystallization (cooling) occurred. This profile was

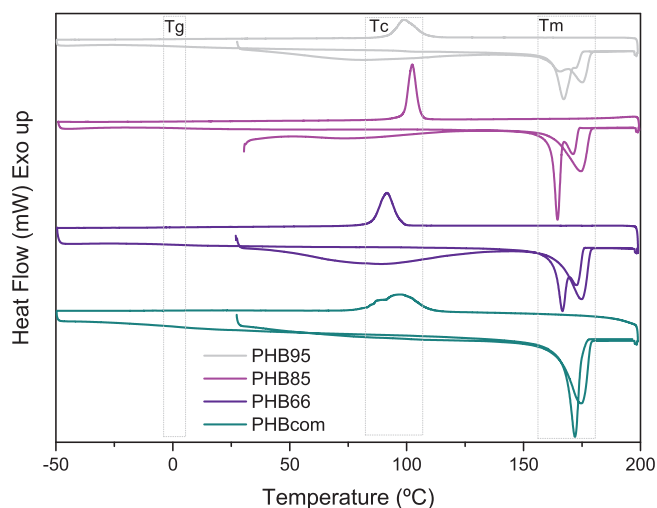


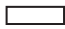



Fig. 5. DSC thermograms of extracted (PHB66) and successively purified (PHB85 and PHB95) PHB samples. A commercial PHB (PHBcom) was used as comparison.

to obtain PHB95 samples as films, while PHB66 and PHB 85 samples were obtained as powder.

The main parameters resulting from TGA and derivative curves (DTG) are summarized in Table 2. The onset temperature (T_{onset}) and its mass loss varied by ~20 °C and ~40 %, respectively, while the maximum thermal decomposition (T_{max}) of the biopolymer (known as

Table 4

Colour parameters (L^* , a^* , and b^*) of extracted (PHB66) and purified (PHB85 and PHB95) PHB samples. A commercial PHB (PHBcom) was used for comparison.

Sample	L^*	a^*	b^*	Colour (RGB)
PHBcom	101.3 ± 0.9^a	-0.1 ± 0.0^a	0.6 ± 0.1^a	
PHB66	47.3 ± 1.1^b	2.2 ± 0.1^b	0.9 ± 0.1^a	
PHB85	74.4 ± 2.0^c	2.9 ± 0.1^c	3.2 ± 0.1^b	
PHB95	87.2 ± 0.5^d	1.7 ± 0.1^d	1.6 ± 0.2^c	

Two means followed by the same letter in the same column are not significantly ($P > 0.05$) different through Tukey's multiple range test.

linked in the literature to the presence of different crystal sizes [38]. As for T_g , the lowest values were found in PHB66, which could be related to the presence of impurities, such as the aromatic compounds found via 1H NMR and FTIR results. The impurities might have eased the mobility of polymer chains in the amorphous region of the PHB, and thus reduced the T_g of the sample. However, as the purification processes were undertaken, the T_g values of the PHB85 and PHB95 samples increased to values close to $5^\circ C$. These values were $2.3^\circ C$ higher than those of the PHBcom used for comparison. Nevertheless, the thermal behaviour of the extracted and purified biopolymers was consistent with the pattern presented by PHBcom. In addition, similar T_m , T_c and T_g values can be found in the literature [11,32,39]. Regarding the crystallinity of the

biopolymers, the presence of T_m and T_c can be linked to the XRD results, which suggested that the PHBs had a crystalline structure. The crystallinity values obtained by DSC (X_c) showed the same trend as those of XRD (CrI), where the lowest crystallinity was observed in the most purified PHB sample (PHB95).

3.6. Colour

The effect of the purification processes on the colour of the PHBs was analysed using a colourimeter and the results are displayed in Table 4. The removal of impurities notably whitened the samples from a dark grey-coloured product (not purified PHB66) to a light grey-coloured sample (PHB95) as more purification steps were undertaken. This was mainly seen by the increase in the L^* colour parameter value, as well as by the changes in a^* and b^* values. A whitening effect of the purification process was also observed by de Souza Reis and co-workers [40] for the purification of a PHA with 1-butanol. The purification processes in this study, however, did not provide the samples with the same whiteness as the commercial PHB sample (PHBcom).

3.7. Release of compounds and antioxidant activity

The migration of components from the PHB66 sample into 3 different food simulants (MQW, 50EtOH and 95EtOH) is shown in Fig. 6a. The release increased as the hydrophilic character of the food simulants

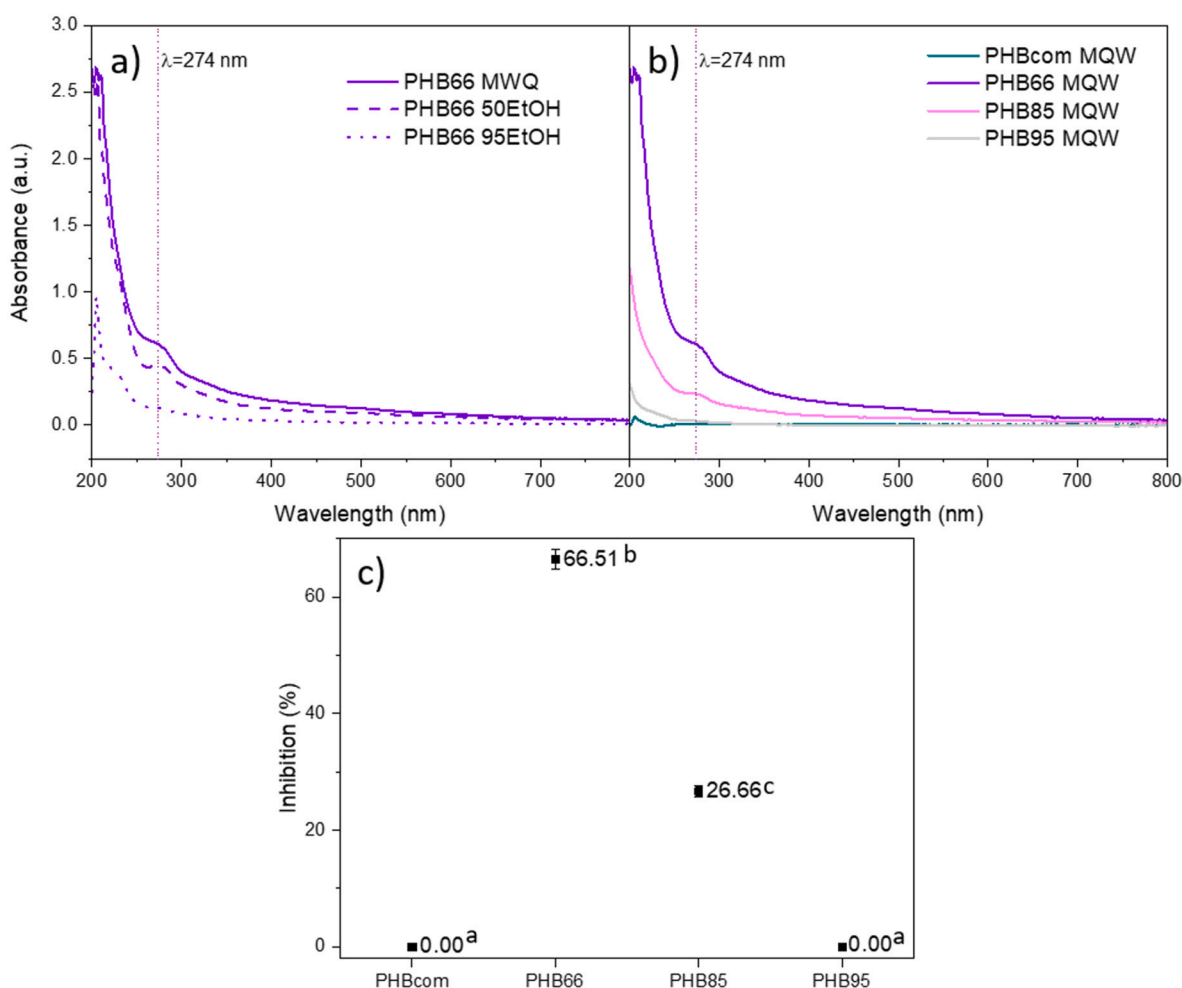


Fig. 6. a) Release of compounds from PHB66 into different food simulants: Milli-Q water (MQW), 50 % v/v ethanol (50EtOH) and 95EtOH; b) release of compounds from extracted (PHB66) and successively purified (PHB85 and PHB95) PHB samples into MQW; and c) antioxidant activity (inhibition, %) of compounds released from the PHB samples into MQW. A commercial PHB (PHBcom) was used for comparison. Two means followed by the same letter are not significantly ($P > 0.05$) different through Tukey's multiple range test.

increased (MQW > 50EtOH > 95EtOH). This result means that the aromatic impurities in the extracted samples (PHB66) were mainly hydrophilic rather than lipophilic substances, which mainly absorbed UV light in the 200 to 350 nm range. It is well known that phenolic compounds in the grape marc, such as gallic acid, catechin and quercetin, present wavelengths of a maximum absorbance around 274 nm, 280 nm, and 375 nm respectively [41–43]. Further, the presence of peptide bonds, as well as chromophores such as tyrosine and phenylalanine (common aromatic amino acids found in proteins), can be found between 200 and 300 nm [44]. Therefore, along with the ¹H NMR and FTIR results, the release data also confirmed the presence of aromatic impurities in the extracted PHB66 sample.

Considering that MQW was able to extract more components from the PHB66 sample than the lipophilic food simulants, MQW was used to conduct release and antioxidant studies with all of the PHB samples (Fig. 6 b and c). As can be seen, the released components decreased as the purification of PHB samples increased, and the PHB95 and PHBcom showed no release. This was related to the purification processes conducted on PHB66 to obtain a more pure biopolymer after EtOH washing (PHB85) and a less coloured PHB after immersion of PHB85 in CHCl₃ (PHB95). Therefore, purification processes removed impurities from the extracted PHB sample (PHB66) and, as a result, the PHB biopolymer reduced (PHB85) or lost (PHB95) its antioxidant activity (Fig. 6c). These results indicated that the released compounds presented antioxidant activity, as shown by the inhibition values in Fig. 6c (PHB66 > PHB85 > PHB95 = PHBcom). Therefore, the release compounds were antioxidant compounds that could migrate from the PHB sample into a hydrophilic environment (MQW), a desirable property for materials intended to be used in food packaging applications, especially in active packaging, as well as in biomedical applications where biomaterials with antioxidant properties are needed.

4. Conclusions

The PHA synthesized by strain *Cupriavidus necator* H 1 G⁺3 was confirmed to be PHB as seen via ¹H NMR and FTIR results. These outcomes also showed the presence of amino acids and aromatic compounds found in by-products from winemaking processes (grape pomace extracts). The presence of those compounds decreased with PHB purification steps. Consequently, the colour of PHB samples became whiter/clearer and amount of released components from the biopolymer into food simulants decreased. Furthermore, these released compounds presented antioxidant activity, a desirable property for materials intended to be used in food packaging and biomedical applications, which could help avoid the further use of (synthetic) antioxidant additives. Regarding the crystallinity observed by XRD and DSC analyses, a reduction was observed with further purification steps. Since the lower crystallinity of the polymers is linked to less brittle properties, this reduction would increase the range of applications of the PHB-based material. Additionally, the PHBs produced in this study had high thermal stability regardless of their purification level. Although further studies are needed for specific applications, taking the abovementioned results into consideration, PHB85 samples could be a potential alternative to reduce the use of synthetic polymers since with this intermediate purification process, the production process is shorter and the crystallinity is reduced, while the antioxidant activity is maintained.

CRedit authorship contribution statement

Alaitz Etxabide: Conceptualization, Methodology, Validation, Investigation, Writing - Original Draft, Visualisation, Writing - Review & Editing; **Paul A. Kilmartin:** Writing - Review & Editing, Supervision, Funding acquisition; **Pedro Guerrero:** Writing - Review & Editing, Funding acquisition; **Koro de la Caba:** Writing - Review & Editing, Supervision, Funding acquisition; **David O. Hooks:** Conceptualization, Methodology, Validation, Investigation, Writing - Review & Editing;

Mark West: Conceptualization, Methodology, Validation, Investigation, Writing - Review & Editing; **Tripti Singh:** Writing - Review & Editing, Supervision, Funding acquisition.

Declaration of competing interest

None.

Acknowledgement

The authors would like to thank the Ministry of Business, Innovation and Employment of New Zealand (MBIE, Biocide Toolbox programme), the Basque Government (KK-2021/00131 and IT1658-22) and PID2021-124294OB-C22 project funded by MCIN/AEI/10.13039/501100011033/FEDER, UE. A.E. thanks the State Research Agency of Spain within the Juan de la Cierva - Incorporation action (IJ2019-039697I).

References

- [1] R.E. Martínez-Herrera, M.E. Alemán-Huerta, P. Flores-Rodríguez, V. Almaguer-Cantú, R. Valencia-Vázquez, W. Rosas-Flores, H. Medrano-Roldán, L.A. Ochoa-Martínez, O.M. Rutiaga-Quinones, Utilization of Agave durangensis leaves by *Bacillus cereus* 4N for polyhydroxybutyrate (PHB) biosynthesis, *Int. J. Biol. Macromol.* 175 (2021) 199–208, <https://doi.org/10.1016/j.ijbiomac.2021.01.167>.
- [2] K.Y. Sen, S. Baidurah, Renewable biomass feedstocks for production of sustainable biodegradable polymer, *Curr. Opin. Green Sustain. Chem.* 27 (2021), 100412, <https://doi.org/10.1016/j.cogsc.2020.100412>.
- [3] A. Etxabide, J. Uranga, P. Guerrero, K. de la Caba, Development of active gelatin films by means of valorisation of food processing waste: a review, *Food Hydrocol.* 68 (2017) 192–198, <https://doi.org/10.1016/j.foodhyd.2016.08.021>.
- [4] R.G. Saratale, S.K. Cho, G.D. Saratale, G.S. Ghodake, R.N. Bharagava, D.S. Kim, et al., Efficient bioconversion of sugarcane bagasse into polyhydroxybutyrate (PHB) by *lysibacillus* sp. and its characterization, *Bioresour. Technol.* 324 (2021), 124673, <https://doi.org/10.1016/j.biortech.2021.124673>.
- [5] R. Sirohi, Sustainable utilization of food waste: production and characterization of polyhydroxybutyrate (PHB) from damaged wheat grains, *Environ. Technol. Innov.* 23 (2021), 101715, <https://doi.org/10.1016/j.eti.2021.101715>.
- [6] New Zealand Winegrowers, New Zealand Winegrowers sustainability report. <https://www.nzwine.com/en/sustainability/sustainability-report/>, 2016.
- [7] New Zealand Winegrowers, Vineyard report New Zealand Winegrowers I 2020-2023. <https://www.nzwine.com/media/19216/vineyard-report-2021.pdf>, 2021.
- [8] C.M. Galanakis (Ed.), Handbook of Grape Processing By-Products, Academic Press, 2017, <https://doi.org/10.1016/B978-0-12-809870-7.00016-8>.
- [9] A.A. Kovalcik, I. Pernicova, S. Obruca, M. Sztokowski, V. Enev, M. Kalina, et al., Grape winery waste as a promising feedstock for the production of polyhydroxyalkanoates and other value-added products, *Food Bioprod. Process.* 124 (2020) 1–10, <https://doi.org/10.1016/j.fbp.2020.08.003>.
- [10] R. Sirohi, A. Tarafdar, S. Singh, T. Negi, V.K. Gaur, E. Gnansounou, B. Bharathiraja, Green processing and biotechnological potential of grape pomace: current trends and opportunities for sustainable biorefinery, *Bioresour. Technol.* 314 (2020), 123771, <https://doi.org/10.1016/j.biortech.2020.123771>.
- [11] S. Pradhan, A.J. Borah, M.K. Poddar, P.K. Dikshit, L. Rohidas, V.S. Moholkar, Microbial production, ultrasound-assisted extraction and characterization of biopolymer polyhydroxybutyrate (PHB) from terrestrial (*P. hysterophorus*) and aquatic (*E. crassipes*) invasive weeds, *Bioresour. Technol.* 242 (2017) 304–310, <https://doi.org/10.1016/j.biortech.2017.03.117>.
- [12] M.R. Roohi, M. Zaheer, Kuddus, PHB (poly-β-hydroxybutyrate) and its enzymatic degradation, *Polym. Adv. Technol.* 29 (2018) 30–40, <https://doi.org/10.1002/pat.4126>.
- [13] F.G. Blanco, N. Hernández, V. Rivero-Buceta, B. Maestro, J.M. Sanz, A. Mato, et al., From residues to added-value bacterial biopolymers as nanomaterials for biomedical applications, *Nanomaterials* 11 (2021) 1492, <https://doi.org/10.3390/nano11061492>.
- [14] M. Koller, A. Mukherjee, A new wave of industrialization of PHA biopolyesters, *Bioengineering* 9 (2022) 74, <https://doi.org/10.3390/bioengineering9020074>.
- [15] M.T. Cesário, R.S. Raposo, M. de Almeida, M.D. Catarina, F. van Keulen, B. S. Ferreira, M. da Fonseca, R. Manuela, Enhanced bioproduction of poly-3-hydroxybutyrate from wheat straw lignocellulosic hydrolysates, *New Biotechnol.* 31 (2014) 104–113, <https://doi.org/10.1016/j.nbt.2013.10.004>.
- [16] L. Wei, A.G. McDonald, N.M. Stark, Grafting of bacterial polyhydroxybutyrate (PHB) onto cellulose via in situ reactive extrusion with dicumyl peroxide, *Biomacromolecules* 16 (2015) 1040–1049, <https://doi.org/10.1021/acs.biomac.5b00049>.
- [17] R.E. Martínez-Herrera, M.E. Alemán-Huerta, V. Almaguer-Cantú, W. Rosas-Flores, V.J. Martínez-Gómez, I. Quintero-Zapata, G. Rivera, O.M. Rutiaga-Quinones, Efficient recovery of thermostable polyhydroxybutyrate (PHB) by a rapid and solvent-free extraction protocol assisted by ultrasound, *Int. J. Biol. Macromol.* 164 (2020) 771–782, <https://doi.org/10.1016/j.ijbiomac.2020.07.101>.

- [18] A.D. Tripathi, T. Raj Joshi, S. Kumar Srivastava, K.K. Darani, S. Khade, J. Srivastava, Effect of nutritional supplements on bio-plastics (PHB) production utilizing sugar refinery waste with potential application in food packaging, *Prep. Biochem. Biotechnol.* 49 (2019) 567–577, <https://doi.org/10.1080/10826068.2019.1591982>.
- [19] S. Maity, S. Das, S. Mohapatra, A.D. Tripathi, J. Akthar, S. Pati, et al., Growth associated polyhydroxybutyrate production by the novel *Zobellella tiwanensis* strain DD5 from banana peels under submerged fermentation, *Int. J. Biol. Macromol.* 153 (2020) 461–469, <https://doi.org/10.1016/j.ijbiomac.2020.03.004>.
- [20] (EU) No 10/2011, Commission Regulation (EU) No 10/2011 of 14 January 2011 on plastic materials and articles intended to come into contact with food. <https://eur-lex.europa.eu/legal-content/EN/ALL/?uri=celex%3A32011R0010>, 2011.
- [21] M.R. Khan, F.A. Di Giuseppe, E. Torrieri, M.B. Sadiq, Recent advances in biopolymeric antioxidant films and coatings for preservation of nutritional quality of minimally processed fruits and vegetables, *Food Packag. Shelf Life* 30 (2021), 100752, <https://doi.org/10.1016/j.fpsl.2021.100752>.
- [22] A. Etxabide, V. Coma, P. Guerrero, C. Gardrat, K. de la Caba, Effect of cross-linking in surface properties and antioxidant activity of gelatin films incorporated with a curcumin derivative, *Food Hydrocoll.* 66 (2017) 168–175, <https://doi.org/10.1016/j.foodhyd.2016.11.036>.
- [23] C. Trakunjae, A. Boondaeng, W. Apiwatanapiwat, A. Kosugi, T. Arai, K. Sudesh, P. Vaithanomsat, Enhanced polyhydroxybutyrate (PHB) production by newly isolated rare actinomycetes *rhodococcus* sp. Strain BSRT1-1 using response surface methodology, *Sci. Rep.* 11 (2021) 1896, <https://doi.org/10.1038/s41598-021-81386-2>.
- [24] M. Narayanan, G. Kandasamy, P. Murali, S. Kandasamy, V. Ashokkumar, O. Nasif, A. Pugazhendhi, Optimization and production of polyhydroxybutyrate from sludge by *Bacillus cereus* categorized through FT-IR and NMR analyses, *J. Environ. Chem. Eng.* 9 (2021), 104908, <https://doi.org/10.1016/j.jece.2020.104908>.
- [25] O. Vega-Castro, J. Contreras-Calderon, E. León, A. Segura, M. Arias, L. Pérez, P. J. Sobral, Characterization of a polyhydroxyalkanoate obtained from pineapple peel waste using *Ralstonia eutropha*, *J. Biotechnol.* 231 (2016) 232–238, <https://doi.org/10.1016/j.jbiotec.2016.06.018>.
- [26] C. Phithakrotchanakoon, V. Champreda, S. Aiba, K. Pootanakit, S. Tanapongpipat, Production of polyhydroxyalkanoates from crude glycerol using recombinant *Escherichia coli*, *J. Polym. Environ.* 23 (2015) 38–44, <https://doi.org/10.1007/s10924-014-0681-8>.
- [27] G. Carullo, A. Ahmed, F. Fusi, F. Sciubba, M.E. Di Cocco, D. Restuccia, et al., Vasorelaxant effects induced by red wine and pomace extracts of *magliocco dolce* cv, *Pharmaceuticals*. 13 (2020) 87, <https://doi.org/10.3390/ph13050087>.
- [28] B. Hu, J. Gao, S. Xu, J. Zhu, X. Fan, X. Zhou, Quality evaluation of different varieties of dry red wine based on nuclear magnetic resonance metabolomics, *Appl. Biol. Chem.* 63 (2020) 24, <https://doi.org/10.1186/s13765-020-00509-x>.
- [29] S. Bayan, F. Severcan, FTIR study of biodegradable biopolymers: P(3HB), P(3HB-co-4HB) and P(3HB-co-3HV), *J. Mol. Struct.* 744–747 (2005) 529–534, <https://doi.org/10.1016/j.molstruc.2004.12.029>.
- [30] A. Barth, The infrared absorption of amino acid side chains, *Prog. Biophys. Mol. Biol.* 74 (2000) 141–173, [https://doi.org/10.1016/S0079-6107\(00\)00021-3](https://doi.org/10.1016/S0079-6107(00)00021-3).
- [31] M. Lucarini, A. Durazzo, J. Kiefer, A. Santini, G. Lombardi-Boccia, E.B. Souto, et al., Grape seeds: chromatographic profile of fatty acids and phenolic compounds and qualitative analysis by FTIR-ATR spectroscopy, *Foods* 9 (2020) 10, <https://doi.org/10.3390/foods9010010>.
- [32] S. Pradhan, P.K. Dikshit, V.S. Moholkar, Production, ultrasonic extraction, and characterization of poly (3-hydroxybutyrate) (PHB) using *Bacillus megaterium* and *Cupriavidus necator*, *Polym. Adv. Technol.* 29 (2018) 2392–2400, <https://doi.org/10.1002/pat.4351>.
- [33] R.G. Saratale, S. Cho, G.S. Ghodake, H. Shin, G.D. Saratale, Y. Park, et al., Utilization of noxious weed water hyacinth biomass as a potential feedstock for biopolymers production: a novel approach, *Polymers* 12 (2020) 1704, <https://doi.org/10.3390/polym12081704>.
- [34] D. Briassoulis, P. Tserotas, I. Athanasoulia, Alternative optimization routes for improving the performance of poly(3-hydroxybutyrate) (PHB) based plastics, *J. Clean. Prod.* 318 (2021), 128555, <https://doi.org/10.1016/j.jclepro.2021.128555>.
- [35] K. Dietrich, M. Dumont, V. Orsat, L.F. Del Rio, In-depth material characterization of polyhydroxybutyrate from a forest biorefinery, *J. Appl. Polym. Sci.* 138 (2021) 51375, <https://doi.org/10.1002/app.51375>.
- [36] M. Niaoounakis, Chapter 2 - properties, in: M. Niaoounakis (Ed.), *Biopolymers: Processing and Products*, William Andrew Publishing, Oxford, 2015, pp. 79–116, <https://doi.org/10.1016/B978-0-323-26698-7.00002-7>.
- [37] C. Sanhueza, P. Diaz-Rodriguez, P. Villegas, Á. González, M. Seeger, J. Suárez-González, A. Concheiro, C. Alvarez-Lorenzo, F. Acevedo, Influence of the carbon source on the properties of poly-(3)-hydroxybutyrate produced by *paraburkholderia xenovorans* LB400 and its electrospun fibers, *Int. J. Biol. Macromol.* 152 (2020) 11–20, <https://doi.org/10.1016/j.ijbiomac.2020.02.080>.
- [38] da Silva, L.R. de Menezes, Paulo Sérgio R.C. da Silva, M.I.B. Tavares, Evaluation of thermal properties of zirconium-PHB composites, *J. Therm. Anal. Calorim.* 143 (2021) 165–172, <https://doi.org/10.1007/s10973-019-09106-7>.
- [39] S. Ansari, T. Fatma, Cyanobacterial polyhydroxybutyrate (PHB): screening, optimization and characterization, *PLoS ONE* 11 (2016), e0158168, <https://doi.org/10.1371/journal.pone.0158168>.
- [40] A. Guilherme, Reis de Souza, M.H.A. Michels, G.L. Fajardo, I. Lamot, J.H. de Best, Optimization of green extraction and purification of PHA produced by mixed microbial cultures from sludge, *Water* 12 (2020) 1185, <https://doi.org/10.3390/w12041185>.
- [41] M. Stevenson, J. Long, P. Guerrero, K.D.L. Caba, A. Seyfoddin, A. Etxabide, Development and characterization of ribose-crosslinked gelatin products prepared by indirect 3D printing, *Food Hydrocoll.* 96 (2019) 65–71, <https://doi.org/10.1016/j.foodhyd.2019.05.018>.
- [42] F. Luzzi, E. Pannucci, L. Santi, J.M. Kenny, L. Torre, R. Bernini, et al., Gallic acid and quercetin as intelligent and active ingredients in Poly(vinyl alcohol) films for food packaging, *Polymers* 11 (2019) 1999, <https://doi.org/10.3390/polym11121999>.
- [43] M.P. Arrieta, A. Díez García, D. López, S. Fiori, L. Peponi, Antioxidant bilayers based on PHBV and plasticized electrospun PLA-PHB fibers encapsulating catechin, *Nanomater.* 9 (2019) 346, <https://doi.org/10.3390/nano9030346>.
- [44] J. Bonilla, P.J.A. Sobral, Investigation of the physicochemical, antimicrobial and antioxidant properties of gelatin-chitosan edible film mixed with plant ethanolic extracts, *Food Biosci.* 16 (2016) 17–25, <https://doi.org/10.1016/j.fbio.2016.07.003>.